Whole-body MRI evaluation of facioscapulohumeral muscular dystrophy

Doris G. Leung, M.D.[1,2], **John A. Carrino, M.D., M.P.H.**[4,6], **Kathryn R. Wagner, M.D., Ph.D.** [1,2,3], and **Michael A. Jacobs, Ph.D.**[4,5]

[1]The Hugo W. Moser Research Institute, Kennedy Krieger Institute, Baltimore, MD

[2]Department of Neurology, Johns Hopkins University School of Medicine, Baltimore, MD

[3]Department of Neuroscience, Johns Hopkins University School of Medicine, Baltimore, MD

[4]Department of Radiology and Radiological Science, Johns Hopkins University School of Medicine, Baltimore, MD

[5]Department of the Sidney Kimmel Cancer Center, Johns Hopkins University School of Medicine, Baltimore, MD

[6]Department of Radiology and Imaging, Hospital for Special Surgery, New York, NY

Abstract

Introduction—Facioscapulohumeral muscular dystrophy (FSHD) is a hereditary disorder that causes progressive muscle wasting. Increasing knowledge of the pathophysiology of FSHD has stimulated interest in developing biomarkers of disease severity.

Methods—Two groups of MRI scans were analyzed: whole-body scans from 13 subjects with FSHD, and upper and lower extremity scans from 34 subjects with FSHD who participated in the MYO-029 clinical trial. Muscles were scored for fat infiltration and edema-like changes. Fat infiltration scores were compared to muscle strength and function.

Results—Our analysis reveals a distinctive pattern of both frequent muscle involvement and frequent sparing in FSHD. Averaged fat infiltration scores for muscle groups in the legs correlated with quantitative muscle strength and 10-meter walk times.

Discussion—Advances in MRI technology allow for the acquisition of rapid, high-quality whole-body imaging in diffuse muscle disease. This technique offers a promising disease biomarker in FSHD and other muscle diseases.

Keywords

facioscapulohumeral muscular dystrophy; FSHD; whole-body imaging; MRI; radiographic biomarkers

Corresponding author information: Doris G. Leung, M.D., Center for Genetic Muscle Disorders, Kennedy Krieger Institute, 707 North Broadway, 400A, Baltimore, MD 21205, Telephone: (443)923-9525, Fax: (443)923-9515, leungd@kennedykrieger.org.

Introduction

The muscular dystrophies are a class of more than 30 hereditary disorders that cause progressive skeletal muscle wasting and weakness. The progressive disability caused by these disorders leads to a high burden of disease, both in terms of medical comorbidity and cost of care.(1-3) Although great progress has been made in genetic characterization of these disorders, medical treatments are very limited. The promise of future treatment compels us to seek new methods to measure and monitor these disorders during clinical trials and observational studies. The most commonly used outcome measures in muscular dystrophies have significant limitations in their ability to accurately gauge the global disease state.(4) Muscle biopsies sample only small amounts of muscle at a time, and the yield can be inconsistent because muscle involvement can be heterogeneous both within and between muscles. Furthermore, the invasiveness of a muscle biopsy can increase the potential risk to participants, thereby impeding recruitment. Creatine kinase, an intracellular muscle enzyme, is also an inadequate biomarker for trials, because it is not uniformly abnormal in the disease state and can be modified by activity status and muscle mass and thus does not accurately reflect disease severity. Even clinical measures of function and patient-reported outcomes can be confounded heavily by factors that are not related to the disease.(5) Functional measurements, such as the 6-minute walk test, may also change too slowly over the course of a disease to be useful in most clinical trials.(6, 7) Thus, identification of responsive and reproducible biomarkers is a major unmet need in muscular dystrophy research.

Magnetic resonance imaging (MRI) is being recognized increasingly as a noninvasive diagnostic and monitoring tool in skeletal muscle disease due to its excellent measurement of soft tissue characteristics, safety profile, and recent technical advances.(8-10) Although morphologic MRI has been used as an outcome measure in clinical research in myopathies, (11, 12) scans are often limited to localized anatomic structures (for instance, to the lower extremities) due to time constraints. The use of whole-body MRI (WBMRI) overcomes this problem by allowing for interrogation of multiple regions within the body in a clinically feasible time (typically 1 hour or less).(13)

WBMRI may be particularly useful for detection and characterization of skeletal muscle pathology in facioscapulohumeral muscular dystrophy (FSHD), one of the most common forms of muscular dystrophy. Clinically, FSHD causes slowly progressive muscle weakness that preferentially affects the face, shoulder girdle, and ankle dorsiflexors, and muscle involvement can be highly variable between individuals.(14) The available data on muscle imaging in FSHD suggests that subclinical disease is detectable using localized MRI.(15-17) T1-weighted imaging has been used to identify the degree of muscle replacement by fat, and hyperintensity on fluid-sensitive MRI sequences has been shown to represent an active inflammatory phase that precedes fat infiltration.(18-21) The ability to detect these subclinical changes is an important advancement towards clinical trial preparedness in FSHD. A radiological biomarker that is both noninvasive and sensitive to changing severity in a slowly progressive disorder like FSHD could not only improve our understanding of the disease and its progression within the body, but also facilitate quicker clinical trials with smaller sample sizes.

In order to evaluate the feasibility of performing whole-body MRI in FSHD, we performed a cross-sectional pilot study of adults with a wide spectrum of disease severity. The resulting images were used to provide descriptive data on the pattern of muscle involvement in FSHD and to analyze the relationship between clinical and imaging measurements.

Methods

Study design and setting

This study was approved by the Johns Hopkins School of Medicine Institutional Review Board. Adults with FSHD were invited to participate in a single-center, cross-sectional observational study. Study participation consisted of an outpatient clinic visit and MRI scan. The clinic visits were conducted at the Kennedy Krieger Outpatient Clinic, and MRI scans were performed at the Johns Hopkins Hospital (both facilities are located in Baltimore, Maryland). Study participants were enrolled between June 1, 2013 and March 30, 2014.

Recruitment of study participants

Study participants were recruited through IRB-approved announcements in the newsletter of the FSH Society, Inc., through the clinicaltrials.gov registry (NCT01671865), and from the clinic population of the Center for Genetic Muscle Disorders at the Kennedy Krieger Institute. Written informed consent was obtained from each participant prior to enrollment. All participants had previously undergone genetic testing to detect the deletion in chromosome 4 associated with FSHD. Subjects whose genetic testing predated routine testing for the 4qA haplotype were not asked to undergo repeat testing if they had a clinical presentation consistent with FSHD. However, 2 subjects who were asymptomatic both had confirmatory 4qA haplotype testing. Other inclusion criteria included: age 18 years, ability to ambulate independently, and ability and willingness to give informed consent. Exclusion criteria included standard contraindications to MRI scanning. Participants who had undergone scapular fixation were also excluded, as wires and other implants could create field distortions and artifacts in regions of interest despite being MRI-safe. Contraindications to MRI were ascertained through screening forms and in-person screening assessments performed by radiology personnel immediately prior to scanning.

Clinical data collection

Each enrolled subject was evaluated by a neurologist for clinical data collection prior to MRI. Demographic data (age, gender, race/ethnicity) and results of genetic testing for FSHD were documented. Manual muscle testing (MMT) using the Medical Research Council (MRC) scale was performed for each subject. Quantitative muscle testing (QMT) was performed using a hand-held dynamometer (Chatillon DPP series mechanical force gauge). The maximum voluntary isometric force of shoulder abduction, elbow extension, elbow flexion, hip flexion, knee extension, and knee flexion from the best of 2 trials was recorded for each subject.(22) A 10-meter timed walk was also performed for each subject.

MRI protocol

Magnetic resonance images were acquired using a 3 Tesla Magnetom Tim Trio system (Siemens, Erlangen, Germany) with continuous table movement (CTM). Subjects were

placed in a head-first, supine position, and all images were acquired with the subject in this fixed position. Five radiofrequency coils were placed on the patient: an 8-channel head coil, a neck matrix coil, 2 body matrix coils (1 for the chest and 1 for the abdomen/pelvis) and a peripheral angiography (PA) matrix coil positioned over the legs. Fat-suppressed T1-weighted [repetition time (TR)/echo time (TE)=150/3.69ms, field of view (FOV)=50×50cm^2, matrix size=320×161, inversion time (TI)=220ms, slice thickness=5mm, acquisition time 3:09 minutes] and Short Tau Inversion Recovery (STIR) (TR/TE=1200/86ms, FOV=50×50cm^2, matrix size=256×256, TI=240ms, slice thickness = 4-6mm, acquisition time 4:10 minutes) images were acquired using newly-developed CTM sequences. Both sequences scanned a total length of 1590mm. Images from the thorax and abdomen were acquired during 12-15 second breath-holds to minimize artifact from diaphragm movement.

WBMRI imaging outcomes

Skeletal muscle characteristics for all study participants were scored by a single reviewer (DGL) with 3 years of experience reading musculoskeletal MRIs. All muscles visualized on T1-weighted images were scored for the degree of intramuscular infiltration (which appears dark on fat-suppressed images).(23, 24) Histopathologic studies of FSHD and other muscular dystrophies suggest that these infiltrates are composed primarily of fat, although regions of perimysial and endomysial fibrosis are also interspersed among (and radiographically indistinguishable from) the fatty tissue. (25-27) The scoring scale used to assess fat infiltration was described previously by Mercuri et al. and is summarized in Table 1.(28-30) A minor modification was made to the fat infiltration scale; the additional score level of 5 was added to signify 100% fat infiltration on T1-weighted imaging (examples of fat infiltration scoring are provided in Supplementary Figure 1). This new score level was felt to be biologically significant, as it would define a stage of disease at which no further fat infiltration could occur. For each muscle, the frequency of involvement, the mean fat infiltration score, and the frequency of asymmetric involvement across the study population were calculated. Each of the muscles scored on T1-weighted imaging was classified as either involved/affected (score 2 or higher) or spared (score 0 or 1). Muscle pairs were defined as asymmetric if there was any difference in fat infiltration score between the right and left muscles in a single individual. Muscles were ranked by frequency of involvement, along with the mean fat infiltration scores and the proportion of asymmetric muscle pairs. Muscles visualized on STIR images were scored on a dichotomous scale, with hyperintensity being either present or absent.

Data analysis

Linear regression models were used to study the relationship between clinical outcomes and fat infiltration scores on MRI. Scores for individual muscles comprising the hip flexors (iliopsoas, iliacus, psoas major), quadriceps (vastus lateralis, vastus medialis, vastus intermedius, rectus femoris), hamstrings (semitendinosus, semimembranosus, long and short heads of the biceps femoris), biceps brachii (long and short heads), and deltoids (anterior, medial, and posterior) were averaged to produce a mean fat infiltration score for the muscle group, which was analyzed as the predictor variable. The muscle strength (in pounds) was regressed against the mean fat infiltration scores for different muscles groups using

univariable regression analyses. Univariable and multivariable linear regression models were used to evaluate the associations between 10-meter walk times and mean MRI scores in the hamstrings, hip flexors, and quadriceps (these muscle groups were selected because they were visualized in their entirety in all 13 subjects). All analyses were performed using the Stata 12/IC statistical software package (StataCorp LP, College Station, Texas).(31) Figures were created using both Stata 12/IC and R version 3.1.0.

Replication of MRI scoring technique in a second study population

Given the small sample size in the WBMRI study, we retrospectively analyzed a second collection of MRI scans from a larger series of patients with FSHD. This collection consisted of proton density MRI scans of participants in the MYO-029 trial, a randomized controlled trial of a myostatin inhibitor in subjects with multiple types of muscular dystrophy. Individuals in this study were enrolled at 10 participating centers (9 in the United States and 1 in the United Kingdom). The detailed inclusion and exclusion criteria and methods for acquisition of data for this trial are described elsewhere. (11) Each subject had MRIs of all 4 extremities (1.5 Tesla axial proton density sequences; TE=13.77 ms; TR=6000 ms; number of excitations=1; matrix 256×256; acquisition time 1.2 minutes) and quantitative muscle testing performed prior to initiation of the study drug. These baseline MRI scans were scored for fat infiltration using the same 6-point scale by a single reviewer (DGL).(32, 33) Linear regression analyses were used to examine the association between quantitative muscle strength and mean fat infiltration scores in the quadriceps, hamstring, biceps brachii, and triceps.

Results

Study participants

Thirteen individuals (8 men, 5 women) met all screening criteria and were enrolled in the WBMRI study. The mean age of this study population was 48 years [standard deviation (SD) 14, range 20-72 years]. All subjects completed the study in its entirety, and no complications were reported. For each subject, 92 to 118 pairs of muscles were visualized and scored for fat infiltration and edema-like abnormalities.

Thirty-four individuals with FSHD participated in the MYO-029 trial and had MRI scans and quantitative muscle testing data available for review. Of these individuals, 26 were men, 8 were women. The mean age of this group was 43 years (SD 10, range 21-70). All were ambulatory at the time of study initiation.

Frequency, severity, and distribution of muscle involvement

There was considerable clinical variability in disease severity between subjects in the WBMRI study population, and this is reflected in the percentage of muscles that were affected in individuals; between 3% and 75% of muscles were affected (with fat infiltration scores 2) in the study sample. Asymmetry in muscle groups was a common finding. Over the entire study population, 37.5% of abnormal muscle pairs (either unilaterally or bilaterally) were affected asymmetrically. Tables 2a-c list individual muscles of the upper extremity, lower extremity, and trunk by decreasing frequency of involvement. The most

frequently and severely involved muscle overall was the semimembranosus (24 of 26 muscles visualized were affected; the mean fat infiltration score was 4.04). This is consistent with previously-reported data using localized MRI imaging in FSHD.(34) Muscles of the trunk (including the paraspinal muscles and muscles of the abdominal wall) were also among the muscles involved most frequently (Table 2c). We further identified several muscles that were frequently spared in the study population. The bilateral iliacus, obturator externus, obturator internus, subscapularis, infraspinatus, and teres minor muscles were scored for all 13 subjects and were uniformly spared (defined as affected in 0% of subjects). Preferential muscle involvement and sparing is illustrated in a heat map (Figure 1), which shows fat infiltration scores across the study cohort.

STIR imaging analysis

Only a minority of muscles in each subject (3 - 14 muscles per subject) were hyperintense on STIR imaging. Over the entire study population, only 79 muscles out of 1330 (5.9% of muscles scored, comprised of 29 different muscle types) fell into this classification. These were most frequently the tibialis anterior and the medial gastrocnemius; each of these muscles accounted for 10% of the muscles that were hyperintense on STIR. The long head of the biceps femoris accounted for 8% of hyperintense muscles, and the adductor magnus, vastus medialis, and teres major each accounted for 6% of the hyperintense muscles. Although STIR hyperintensity was associated with all levels of fat infiltration, it was rarely seen in muscles with the highest fat infiltration scores (Table 3).

Associations between MRI scoring and strength

Figure 2 shows quantitative muscle strength (in pounds) for 5 muscle groups plotted against mean fat infiltration scores of those muscle groups. There was a statistically significant relationship between the mean fat infiltration score and muscle strength in the hamstrings; every 1-point increase in the mean fat infiltration score was associated with a 5.18lb decrease in knee flexion strength (P= 0.003, r = -0.56). Knee extension strength was not associated significantly with mean fat infiltration scores less than 2 (P=0.67) in the quadriceps; however, a statistically significant decline in strength was associated with mean MRI scores greater than 2. Within this range, each 1-point increase in mean fat infiltration score was associated with a 12.8lb decline in knee extension strength (P=<0.0001, r=-0.69). Regression analyses of the hip flexors, biceps brachii, and deltoids were not reported due to the limited range of mean fat infiltration scores for these muscle groups; few individuals had mean fat infiltration scores in the higher range, so stable estimates of the relationship between fat infiltration scores and strength could not be obtained. Single linear regression models showed a 0.78 second increase in 10-meter walk time for every 1-point increase in mean fat infiltration score in the hamstrings (P=0.005, Figure 2). However, a multivariable regression model including all 3 muscle groups (quadriceps, hamstrings, and hip flexors) as predictors revealed a statistically significant association (P=0.013) between 10-meter walk times and average fat infiltration scores in the hip flexors only (each 1-point increase in mean fat infiltration score was associated with a 3.7 second increase in 10-meter walk time). In this model, neither the hamstrings (P=0.07) nor the quadriceps (P=0.63) were statistically significantly associated with 10-meter walk time, but analysis of the hamstrings indicated a trend towards significance.

Associations between MRI and strength in the MYO-029 trial

In the MYO-029 data set, a non-linear relationship between muscle strength and mean fat infiltration score was identified in the hamstrings, similar to that seen in the quadriceps (Figure 3). In both the hamstrings and quadriceps, there was no statistically significant change in strength associated with mean fat infiltration scores <2. For mean fat infiltration scores >2, each 1-point increase in mean hamstring fat infiltration score was associated with a 5.9lb decrease in knee flexion strength (P<0.0001, r=-0.80). Likewise, each 1-point increase in mean quadriceps fat infiltration score above 2 was associated with a 9.6lb decrease in knee extension strength (P<0.0001, r=-0.56). In this data set, the hip flexors were not visualized sufficiently to allow for scoring. Fitted regression lines for biceps brachii and triceps strength against mean fat infiltration score in these muscle groups were reasonably linear. In the biceps brachii, each 1-point increase in mean fat infiltration score was associated with a 2.9lb decrease in strength (P<0.0001, r=-0.71). In the triceps, each 1-point increase in mean fat infiltration score was associated with a 1.9lb decrease in strength (P<0.0001, r=-0.56).

Analysis of asymptomatic individuals

Two of the participants in the WBMRI study had positive genetic testing for FSHD but were asymptomatic. One of these participants was a 45 year-old man, and the other was a 52 year-old woman. Both were tested after a first-degree relative was diagnosed with FSHD, and both had normal strength on physical examination. The man was subsequently found to have asymmetric fatty replacement of the right semimembranosus muscle and mild asymmetry of the trapezius muscles. The woman had normal-appearing muscles with the exception of the piriformis, which was absent on the left (Supplementary Figure 2).

Discussion

In this study, we demonstrate the utility of WBMRI in examining global muscle involvement in muscular dystrophy. The use of whole-body imaging in this population provides valuable new information on the distribution of disease by allowing us to evaluate anatomic regions that are commonly affected in FSHD, such as the shoulder girdle and the trunk, but are rarely imaged in their entirety and cannot be tested individually using manual or quantitative muscle strength testing. The wide spectrum of disease severity captured using WBMRI in this study sample illustrates the heterogeneity of muscle involvement in FSHD that is only partially captured by existing disease biomarkers.

One of the salient findings of this study is that WBMRI can detect muscle involvement before loss of strength is discernible on physical examination. We were able to detect extensive fat infiltration of individual muscles in subjects who had positive genetic testing but were asymptomatic. These findings would not have been detectable without the use of WBMRI. As increasing numbers of mildly affected, pre-symptomatic, or even non-manifesting individuals are identified through genetic testing, imaging may be necessary to accurately characterize their disease.

This study also provides new data regarding the distribution of muscle involvement in FSHD. Severe weakness of some muscles and sparing of others is observed frequently in FSHD.(35, 36) Whole-body imaging in our study population expands upon this observation by identifying severely affected muscles, such as the paraspinal muscles, that cannot be examined easily in a clinical setting. Improved characterization of preferentially affected muscles may prove useful in elucidating the pathophysiology that produces the unique clinical findings in FSHD. Distinctive patterns of muscle involvement have been described in imaging studies of other muscular dystrophies and inflammatory muscle disorders, and detailed characterization of these patterns could serve as a diagnostic tool for evaluation of these complex disorders.(37, 38)

The pattern of muscle involvement and sparing that we observe using WBMRI also provides indirect information about the natural history of FSHD. Although the order of muscle involvement cannot be determined definitively in a cross-sectional study, we could reasonably assume that muscles that are affected most frequently across the study population are affected earlier in the disease process. The frequent involvement of the hamstring muscles, for instance, suggests that they are among the earliest muscles affected in FSHD, but the experience of our center is that knee flexion weakness is rarely an early clinical complaint. This is likely due to sparing of the remaining muscles in that muscle group. These results also suggest that progression of fat infiltration to the remaining hamstring muscles is associated with decline in muscle strength. A non-invasive predictor of clinical change would be a valuable tool for monitoring disease progression in observational studies and clinical trials in FSHD. The ability to obtain a global view of all muscle groups in a single setting with WBMRI would also enable us to better understand the relationship between clinical and subclinical manifestations of the disease.

Prior studies have indicated that there is an active phase of inflammatory muscle disease characterized by edema-like changes on fluid-sensitive MRI sequences (e.g. STIR), and that this phase is followed by rapid fat replacement.(18, 20) Indirect evidence for the phenomenon comes from the distribution of fat infiltration scores in this and other studies. (39) Larger proportions of muscles were either severely affected or unaffected, while a relative minority of muscles fell in the intermediate levels (between 30-60%) of fat replacement (Table 3). This distribution suggests that the intermediate phase of muscle replacement occurs rapidly in FSHD, and the limited longitudinal data available in FSHD provides further support for this idea.(39, 40) Longitudinal WBMRI imaging of larger numbers of patients will therefore be an important next step in capturing the distribution of disease across this highly variable disease population and correlating the MRI and clinical phenotypes of FSHD.

There are some notable limitations to this study. Sample size is 1 of the most significant, particularly in a disease with high inter-individual variability. We anticipate that the small sample sizes are the primary reason for the lack of statistically significant relationships between the 10-meter walk times and fat infiltration scores in the quadriceps and hip flexors, as these muscles are likely to be major determinants of walking speed. Additional studies in larger numbers of patients will be crucial for development of any imaging biomarker that we may propose to use in clinical trials. We also excluded non-ambulatory individuals and

individuals who had scapular fixation surgery. Both groups represent more severe phenotypes of FSHD and should be included in future studies. The whole-body imaging technique that we used also placed the arms near the edges of the magnet bore, resulting in distortional artifacts in these regions for a large proportion of subjects.

A second limitation is the use of fat-suppressed T1-weighted imaging to score fat infiltration. Prior studies that have scored fat infiltration in muscle have used non-fat suppressed images, which offer greater contrast between fat and muscle. Non-uniformity of fat suppression during scanning may also affect the appearance of muscles and thereby alter the fat infiltration scoring. In our study sample, only the fat-suppressed sequences were obtained in all 13 participants with sufficient image quality for scoring. Qualitative comparisons of fat-suppressed and non-fat suppressed images (when available) increase our confidence that the fat-suppressed T1 sequences used in this analysis contain sufficient uniformity of fat suppression and contrast for semi-quantitative scoring of fat infiltration (examples are included in Supplementary Figures 1 and 2). Furthermore, analysis of fat infiltration scores from the non-fat suppressed images (available in 7 of the 13 subjects) showed a high level of agreement with scores from the fat suppressed images. Nonetheless, these technical differences may limit the comparability of this study and other imaging studies in FSHD.

Another limitation is the use of a semi-quantitative scoring method. Although the method has been validated in other studies, the potential for inter-interpreter variability and bias is inherent to this type of rating scale. Another disadvantage to this method is the stratification of a continuous parameter (muscle infiltration) into only 6 disease levels, which limits our ability to examine the relationship between muscle strength and fat infiltration within strata. Increasing evidence supports of the use of fully-quantitative imaging techniques and algorithms (such as Dixon imaging) to quantify fat replacement in skeletal muscle.(41) The incorporation of these quantitative measures into whole-body MRI protocols will be an important next step in developing radiological biomarkers for FSHD and other generalized muscle diseases.(42)

Despite these limitations, the wealth of information obtained using a WBMRI approach to FSHD promises new insight into the natural history of FSHD beyond localized imaging and into a more global paradigm. Advanced MRI techniques and technology also provide the opportunity for rapid, standardized acquisition of high-quality images and a platform for the inclusion of novel imaging sequences in future studies of muscle disease.

Supplementary Material

Refer to Web version on PubMed Central for supplementary material.

Acknowledgments

Abbreviations

FSHD	facioscapulohumeral muscular dystrophy
MRI	magnetic resonance imaging
WBMRI	whole-body magnetic resonance imaging
MMT	manual muscle testing
QMT	quantitative muscle testing
CTM	continuous table movement
PA	peripheral angiography
STIR	short tau inversion recovery
TR	repetition time
TE	echo time
FOV	field of view
TI	inversion time
SD	standard deviation

References

1. Ouyang L, Grosse SD, Kenneson A. Health care utilization and expenditures for children and young adults with muscular dystrophy in a privately insured population. Journal of child neurology. 2008; 23(8):883–8. [PubMed: 18403582]

2. Economics, A. Association MD. The Cost of Muscular Dystrophy. Access Economics; 2007.

3. Larkindale J, Yang W, Hogan PF, Simon CJ, Zhang Y, Jain A, et al. Cost of illness for neuromuscular diseases in the United States. Muscle & nerve. 2014; 49(3):431–8. [PubMed: 23836444]

4. Mercuri E, Mayhew A, Muntoni F, Messina S, Straub V, Van Ommen GJ, et al. Towards harmonisation of outcome measures for DMD and SMA within TREAT-NMD; report of three expert workshops: TREAT-NMD/ENMC workshop on outcome measures, 12th--13th May 2007, Naarden, The Netherlands; TREAT-NMD workshop on outcome measures in experimental trials for DMD, 30th June--1st July 2007, Naarden, The Netherlands; conjoint Institute of Myology TREAT-NMD meeting on physical activity monitoring in neuromuscular disorders, 11th July 2007, Paris, France. Neuromuscul Disord. 2008; 18(11):894–903. [PubMed: 18818076]

5. Mazzone ES, Vasco G, Palermo C, Bianco F, Galluccio C, Ricotti V, et al. A critical review of functional assessment tools for upper limbs in Duchenne muscular dystrophy. Developmental medicine and child neurology. 2012; 54(10):879–85. [PubMed: 22713125]

6. Stubgen JP, Stipp A. Facioscapulohumeral muscular dystrophy: a prospective study of weakness and functional impairment. Journal of neurology. 2010; 257(9):1457–64. [PubMed: 20352247]

7. A prospective, quantitative study of the natural history of facioscapulohumeral muscular dystrophy (FSHD): implications for therapeutic trials. The FSH-DY Group. Neurology. 1997; 48(1):38–46. [PubMed: 9008491]

8. Arpan I, Forbes SC, Lott DJ, Senesac CR, Daniels MJ, Triplett WT, et al. T(2) mapping provides multiple approaches for the characterization of muscle involvement in neuromuscular diseases: a cross-sectional study of lower leg muscles in 5-15-year-old boys with Duchenne muscular dystrophy. NMR Biomed. 2013; 26(3):320–8. [PubMed: 23044995]

9. Willcocks RJ, Arpan IA, Forbes SC, Lott DJ, Senesac CR, Senesac E, et al. Longitudinal measurements of MRI-T in boys with Duchenne muscular dystrophy: Effects of age and disease progression. Neuromuscular disorders: NMD. 2014

10. Wokke BH, van den Bergen JC, Versluis MJ, Niks EH, Milles J, Webb AG, et al. Quantitative MRI and strength measurements in the assessment of muscle quality in Duchenne muscular dystrophy. Neuromuscular disorders: NMD. 2014

11. Wagner KR, Fleckenstein JL, Amato AA, Barohn RJ, Bushby K, Escolar DM, et al. A phase I/IItrial of MYO-029 in adult subjects with muscular dystrophy. Ann Neurol. 2008; 63(5):561–71. [PubMed: 18335515]

12. Forbes SC, Walter GA, Rooney WD, Wang DJ, DeVos S, Pollaro J, et al. Skeletal muscles of ambulant children with Duchenne muscular dystrophy: validation of multicenter study of evaluation with MR imaging and MR spectroscopy. Radiology. 2013; 269(1):198–207. [PubMed: 23696684]

13. Jacobs MA, Pan L, Macura KJ. Whole-body diffusion-weighted and proton imaging: a review of this emerging technology for monitoring metastatic cancer. Semin Roentgenol. 2009; 44(2):111–22. [PubMed: 19233086]

14. Tawil R. Facioscapulohumeral muscular dystrophy. Neurotherapeutics. 2008; 5(4):601–6. [PubMed: 19019312]

15. Friedman SD, Poliachik SL, Carter GT, Budech CB, Bird TD, Shaw DW. The magnetic resonance imaging spectrum of facioscapulohumeral muscular dystrophy. Muscle & nerve. 2012; 45(4):500–6. [PubMed: 22431082]

16. Olsen DB, Gideon P, Jeppesen TD, Vissing J. Leg muscle involvement in facioscapulohumeral muscular dystrophy assessed by MRI. Journal of neurology. 2006; 253(11):1437–41. [PubMed: 16773269]

17. Kan, HE.; Janssen, BH.; Voet, NBM. Facioscapulohumeral dystrophy. In: Wattjes, MP.; Fischer, D., editors. Neuromuscular Imaging. New York: Springer; 2013. p. 295-304.

18. Tasca G, Pescatori M, Monforte M, Mirabella M, Iannaccone E, Frusciante R, et al. Different molecular signatures in magnetic resonance imaging-staged facioscapulohumeral muscular dystrophy muscles. PLoS One. 2012; 7(6):e38779. [PubMed: 22719944]

19. Kan HE, Scheenen TW, Wohlgemuth M, Klomp DW, van Loosbroek-Wagenmans I, Padberg GW, et al. Quantitative MR imaging of individual muscle involvement in facioscapulohumeral muscular dystrophy. Neuromuscular disorders: NMD. 2009; 19(5):357–62. [PubMed: 19329315]

20. Friedman SD, Poliachik SL, Otto RK, Carter GT, Budech CB, Bird TD, et al. Longitudinal features of stir bright signal in FSHD. Muscle Nerve. 2013

21. Kan HE, Klomp DW, Wohlgemuth M, van Loosbroek-Wagemans I, van Engelen BG, Padberg GW, et al. Only fat infiltrated muscles in resting lower leg of FSHD patients show disturbed energy metabolism. NMR in biomedicine. 2010; 23(6):563–8. [PubMed: 20175146]

22. Personius KE, Pandya S, King WM, Tawil R, McDermott MP. Facioscapulohumeral dystrophy natural history study: standardization of testing procedures and reliability of measurements. The FSH DY Group. Physical therapy. 1994; 74(3):253–63. [PubMed: 8115459]

23. Mathur S, Lott DJ, Senesac C, Germain SA, Vohra RS, Sweeney HL, et al. Age-related differences in lower-limb muscle cross-sectional area and torque production in boys with Duchenne muscular dystrophy. Archives of physical medicine and rehabilitation. 2010; 91(7):1051–8. [PubMed: 20599043]

24. Finanger EL, Russman B, Forbes SC, Rooney WD, Walter GA, Vandenborne K. Use of skeletal muscle MRI in diagnosis and monitoring disease progression in Duchenne muscular dystrophy.

Physical medicine and rehabilitation clinics of North America. 2012; 23(1):1–10. ix. [PubMed: 22239869]

25. Lin MY, Nonaka I. Facioscapulohumeral muscular dystrophy: muscle fiber type analysis with particular reference to small angular fibers. Brain & development. 1991; 13(5):331–8. [PubMed: 1723849]

26. Mann CJ, Perdiguero E, Kharraz Y, Aguilar S, Pessina P, Serrano AL, et al. Aberrant repair and fibrosis development in skeletal muscle. Skeletal muscle. 2011; 1(1):21. [PubMed: 21798099]

27. Moyer AL, Wagner KR. Regeneration versus fibrosis in skeletal muscle. Curr Opin Rheumatol. 2011; 23(6):568–73. [PubMed: 21934499]

28. Mercuri E, Pichiecchio A, Allsop J, Messina S, Pane M, Muntoni F. Muscle MRI in inherited neuromuscular disorders: past, present, and future. Journal of magnetic resonance imaging: JMRI. 2007; 25(2):433–40. [PubMed: 17260395]

29. Carlo B, Roberta P, Roberto S, Marina F, Corrado A. Limb-girdle muscular dystrophies type 2A and 2B: clinical and radiological aspects. Basic Appl Myol. 2006; 16(1):17–25.

30. Kim HK, Laor T, Horn PS, Racadio JM, Wong B, Dardzinski BJ. T2 mapping in Duchenne muscular dystrophy: distribution of disease activity and correlation with clinical assessments. Radiology. 2010; 255(3):899–908. [PubMed: 20501727]

31. StataCorp. Stata Statistical Software. Release 12. 2011.

32. Sarkozy A, Deschauer M, Carlier RY, Schrank B, Seeger J, Walter MC, et al. Muscle MRI findings in limb girdle muscular dystrophy type 2L. Neuromuscul Disord. 2012; 22(Suppl 2):S122–9. [PubMed: 22980763]

33. Faridian-Aragh N, Wagner KR, Leung DG, Carrino JA. MRI phenotyping of becker muscular dystrophy. Muscle & nerve. 2014

34. Wattjes MP, Kley RA, Fischer D. Neuromuscular imaging in inherited muscle diseases. European radiology. 2010; 20(10):2447–60. [PubMed: 20422195]

35. Tasca G, Monforte M, Iannaccone E, Laschena F, Ottaviani P, Leoncini E, et al. Upper girdle imaging in facioscapulohumeral muscular dystrophy. PloS one. 2014; 9(6):e100292. [PubMed: 24932477]

36. Rijken NH, van der Kooi EL, Hendriks JC, van Asseldonk RJ, Padberg GW, Geurts AC, et al. Skeletal muscle imaging in facioscapulohumeral muscular dystrophy, pattern and asymmetry of individual muscle involvement. Neuromuscul Disord. 2014

37. Kesper K, Kornblum C, Reimann J, Lutterbey G, Schroder R, Wattjes MP. Pattern of skeletal muscle involvement in primary dysferlinopathies: a whole-body 3.0-T magnetic resonance imaging study. Acta neurologica Scandinavica. 2009; 120(2):111–8. [PubMed: 19154541]

38. Kornblum C, Lutterbey G, Bogdanow M, Kesper K, Schild H, Schroder R, et al. Distinct neuromuscular phenotypes in myotonic dystrophy types 1 and 2: a whole body highfield MRI study. Journal of neurology. 2006; 253(6):753–61. [PubMed: 16511650]

39. Janssen BH, Voet NB, Nabuurs CI, Kan HE, de Rooy JW, Geurts AC, et al. Distinct disease phases in muscles of facioscapulohumeral dystrophy patients identified by MR detected fat infiltration. PloS one. 2014; 9(1):e85416. [PubMed: 24454861]

40. Friedman SD, Poliachik SL, Otto RK, Carter GT, Budech CB, Bird TD, et al. Longitudinal features of STIR bright signal in FSHD. Muscle & nerve. 2014; 49(2):257–60. [PubMed: 23720194]

41. Dahlqvist JR, Vissing CR, Thomsen C, Vissing J. Severe paraspinal muscle involvement in facioscapulohumeral muscular dystrophy. Neurology. 2014

42. Wokke BH, Bos C, Reijnierse M, van Rijswijk CS, Eggers H, Webb A, et al. Comparison of dixon and T1-weighted MR methods to assess the degree of fat infiltration in duchenne muscular dystrophy patients. Journal of magnetic resonance imaging: JMRI. 2013; 38(3):619–24. [PubMed: 23292884]
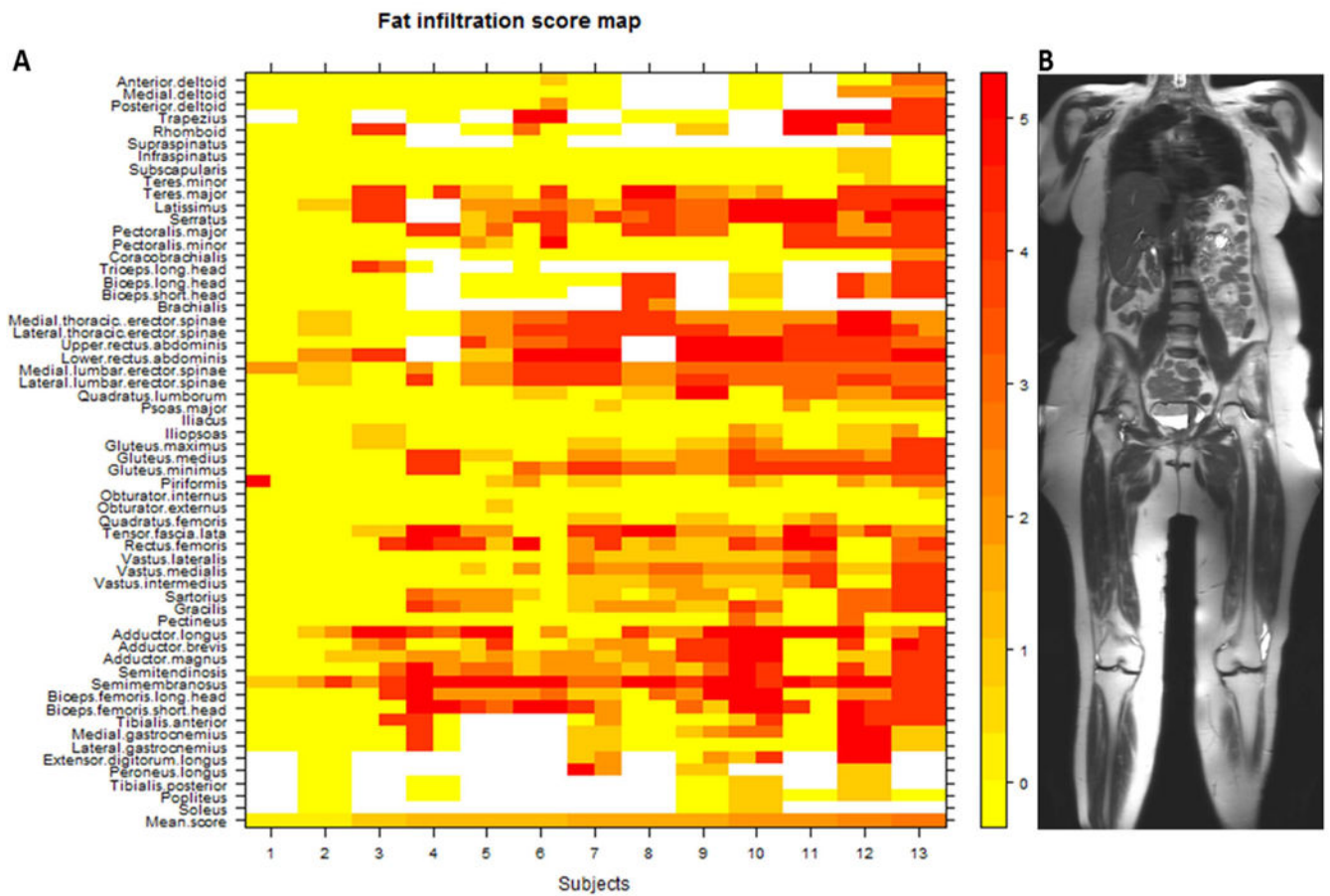
Figure 1.

Heat map (A) of all 1330 muscles scored in 13 individuals with FSHD. Subjects are arranged (left to right) from lowest to highest mean MRI score. Muscles on the left and right sides of the body are placed to the left and right sides (respectively) of the labeled tick marks for each subject. Fat infiltration scores on T1-weighted MRI (from 0 to 5) and their corresponding colors are shown in the numbered bar on the right. The mean MRI score for all muscles scored within a single individual are represented in the bottom row. Muscles are listed in a superior to inferior arrangement, corresponding to the anatomic regions defined by the composite coronal MR image on the right (B).
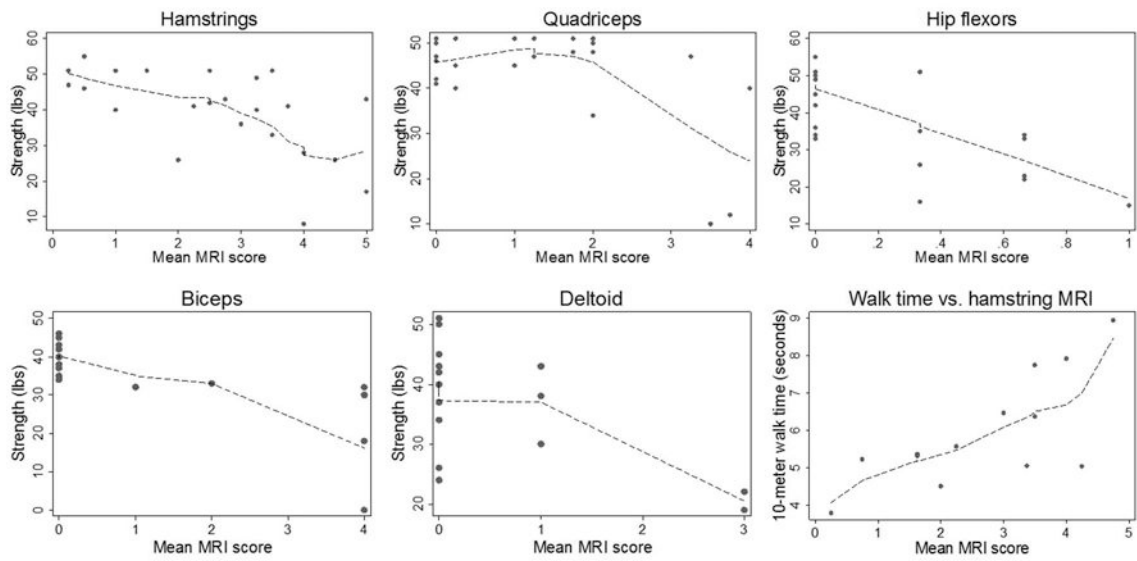
Figure 2.
Fitted regression lines for muscle strength in 5 muscle groups and 10-meter walk time against mean fat infiltration MRI score in specific muscle groups in subjects scanned using whole-body MRI.
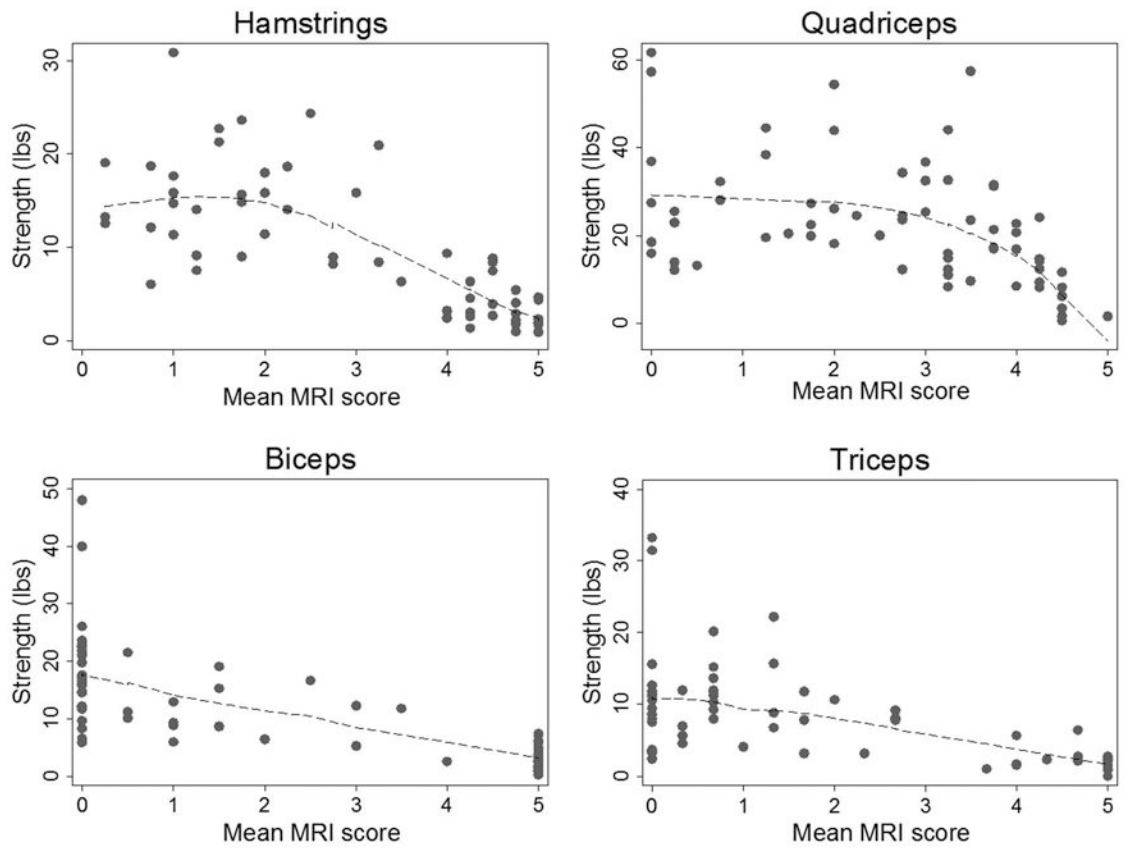
Figure 3.
Fitted regression lines for muscle strength against mean fat infiltration scores on MRI score in specific muscles groups in participants from the MYO-029 trial.

Table 1

MRI scoring parameters.

Score	T1-weighted imaging
0	no fat infiltration
1	trace fat infiltration
2	<30% replacement of muscle with fat
3	30 - <60% replacement of muscle with fat
4	60 - <100% replacement of muscle with fat
5	100% replacement of muscle with fat

Table 2

Table 2a. Frequency, severity, and asymmetry of upper extremity/shoulder girdle muscle involvement observed on T1-weighted WBMRI of 13 individuals with FSHD.

Muscle	Number scored	Percentage affected	Mean fat infiltration score	Percent asymmetric
Pectoralis Major	26	53.8%	1.92	15.4%
Teres Major	26	50.0%	1.96	23.1%
Triceps, Long head	12	33.3%	1.25	16.7%
Biceps, Short head	18	33.3%	1.33	11.1%
Pectoralis Minor	26	30.8%	1.23	15.4%
Biceps, Long head	20	30.0%	1.20	10.0%
Deltoid Middle	20	20.0%	0.40	0.0%
Brachialis	10	20.0%	0.60	20.0%
Deltoid Posterior	18	16.7%	0.56	11.1%
Deltoid, Anterior	20	10.0%	0.35	10.0%
Coracobrachialis	24	8.3%	0.17	0.0%
Supraspinatus	10	0.0%	0.00	0.0%
Infraspinatus	26	0.0%	0.08	0.0%
Subscapularis	26	0.0%	0.08	0.0%
Teres Minor	26	0.0%	0.04	7.7%

Table 2b. Frequency, severity, and asymmetry of lower extremity/hip girdle muscle involvement observed on T1-weighted WBMRI of 13 individuals with FSHD.

Muscle	Number scored	Percentage affected	Mean fat infiltration score	Percent asymmetric
Semimembranosus	26	92.3%	4.04	38.5%
Adductor longus	26	73.1%	2.96	46.2%
Gluteus Minimus	26	69.2%	2.42	7.7%
Tensor fascia lata	26	65.4%	2.31	23.1%
Biceps femoris, long head	26	61.5%	2.08	38.5%
Biceps femoris, short head	26	61.5%	2.62	38.5%
Semitendinosis	26	57.7%	2.00	53.8%
Gluteus Medius	26	53.8%	1.77	15.4%
Rectus femoris	26	53.8%	2.23	61.5%
Vastus medialis	26	50.0%	1.54	38.5%
Gracilis	26	50.0%	1.58	23.1%
Adductor magnus	26	50.0%	1.85	30.8%
Extensor digitorum longus	10	50.0%	2.00	60.0%
Adductor brevis	26	46.2%	1.77	46.2%
Sartorius	26	38.5%	1.23	30.8%
Tibialis anterior	22	36.4%	1.45	45.5%
Medial gastrocnemius	22	27.3%	1.23	18.2%

Table 2b. Frequency, severity, and asymmetry of lower extremity/hip girdle muscle involvement observed on T1-weighted WBMRI of 13 individuals with FSHD.

Muscle	Number scored	Percentage affected	Mean fat infiltration score	Percent asymmetric
Peroneus longus	8	25.0%	1.38	25.0%
Piriformis	26	23.1%	0.85	38.5%
Vastus intermedius	26	23.1%	0.92	23.1%
Vastus lateralis	26	19.2%	0.77	15.4%
Gluteus Maximus	26	15.4%	0.81	7.7%
Lateral gastrocnemius	22	13.6%	0.82	9.1%
Iliopsoas	26	7.7%	0.35	15.4%
Pectineus	26	7.7%	0.27	15.4%
Psoas major	26	3.8%	0.27	15.4%
Quadratus femoris	26	3.8%	0.27	7.7%
Iliacus	26	0.0%	0.00	0.0%
Obturator internus	26	0.0%	0.04	7.7%
Obturator externus	26	0.0%	0.04	7.7%
Tibialis posterior	10	0.0%	0.40	0.0%
Popliteus	14	0.0%	0.29	0.0%
Soleus	6	0.0%	0.33	0.0%

Table 2c. Frequency, severity, and asymmetry of axial muscle involvement observed on T1-weighted WBMRI of 13 individuals with FSHD.

Muscle	Number scored	Percentage affected	Mean fat infiltration score	Percent asymmetric
Lower rectus abdominus	22	81.8%	3.64	0.0%
Lumbar medial erector spinae	26	80.8%	2.38	7.7%
Latissimus dorsi	24	79.2%	3.08	16.7%
Serratus anterior	24	79.2%	3.04	33.3%
Lumbar lateral erector spinae	26	73.1%	2.46	7.7%
Upper rectus abdominus	22	72.7%	2.82	9.1%
Thoracic medial erector spinae	26	69.2%	2.08	0.0%
Thoracic lateral erector spinae	26	69.2%	2.54	7.7%
Trapezius	16	50.0%	2.38	0.0%
Rhomboid	20	40.0%	1.80	20.0%
Quadratus lumborum	26	30.8%	1.23	0.0%

Table 3

Distribution of MRI fat infiltration scores in the whole-body MRI (13 subjects) and MYO-029 (34 subjects) study populations.

Fat infiltration score	Whole-body MRI population (n=1330 scored muscles)	MYO-029 population (n=3126 scored muscles)	Number of STIR hyperintense muscles on WBMRI (n=79 scored muscles)
0	680 (51.1%)	1258 (40.2%)	25 (31.6%)
1	149 (11.2%)	378 (12.1%)	8 (10.1%)
2	136 (10.2%)	275 (8.8%)	18 (22.8%)
3	78 (5.9%)	152 (4.9%)	14 (17.7%)
4	186 (14%)	529 (16.9%)	11 (13.9%)
5	101 (7.6%)	534 (17.1%)	1 (1.3%)